Nuclear Instruments and Methods in Physics Research A 369 (1996) 215–221

ELSEVIER

NUCLEAR INSTRUMENTS & METHODS IN PHYSICS RESEARCH Section A

A computer-controlled tension monitoring system for drift chamber wires

Stephan A. Roth[1], Reinhard A. Schumacher*

Department of Physics, Carnegie Mellon University, Pittsburgh, PA 15213, USA

Received 8 May 1995; revised form received 4 August 1995

Abstract

We describe a wire tension monitor used in the construction and operation of a large drift chamber. This system monitored the tensions of up to 64 wires by locating their resonant frequencies using a sinusoidal current in a weak magnetic field. Wires of 20 μm tungsten and 100 μm aluminum whose lengths varied from 7 to 70 cm were monitored, with resonant frequencies ranging from 160 to 1850 Hz. A multiplexing scheme was implemented which dwelled on each wire for about half a minute. This monitor combined custom electronics with a commercial I/O board and a PC/286 computer. The short-term reproducibility (σ) of the measurements was ±0.05 g (±0.1%) for tungsten wires and 1.1 g (±1.0%) for aluminum wires. Limitations of the method are discussed.

1. Introduction

Sensitive measurements of mechanical tension in the fine wires of a drift chamber are often important to ensure successful construction and operation of these detectors. We describe a system built in conjunction with the innermost tracking drift chamber, "Region One", for the CLAS spectrometer at CEBAF [1]. Over 30 000 wires in this detector were supported by a thin and relatively flexible structure which relied on balanced forces from adjacent sectors of wires for mechanical stability. Controlling these large static forces made careful, quick, and reliable monitoring of mechanical tensions particularly important in this case.

There are several methods and implementations for measuring wire tensions by the detection of resonant frequencies [2]. In all cases the tension, F, is related to the resonant frequency of a wire by the relationship

$$F = \frac{4}{g} L^2 f^2 \mu \,, \tag{1}$$

where L is the length of the wire in meters, f is the fundamental resonant frequency in Hz, and μ is the mass per unit length in grams/meter. Dividing by $g = 9.8\ \mathrm{m/s^2}$ gives F, the mass-equivalent of the tension or force, in grams. In our case the system alternately drove the wire at a trial frequency, then detected the size of the resonant response; the frequency was varied according to a software algorithm to maximize the response. The driving force was generated by a sinusoidal current of typically 30 mA rms in a magnetic field of typically 20 G. The response was detected via the EMF induced in the tested wire as it oscillated freely in the field. The drive signal of 1, 2, 4, or 8 periods of the driving frequency alternated with detection of the response of the wire for a equal length of time.

2. Operation of the computer controlled many-wire tension monitor

Fig. 1 shows a block diagram of our system. At the heart was an IBM-compatible 286 computer with a National Instruments Lab PC+ board [3] for handling the real-time I/O. This board provided 24 channels of digital input/output (DI/O), 8 analog to digital converters (ADCs), 2 digital to analog converters (DACs) and 3 counter/timers. An additional 24 channel DI/O board [3] was used for displaying channel and frequency information on a group of numeric display chips on the front panel of the housing (not shown). The computer controlled the driving frequency and current, the number of periods in the drive and read cycles, and selected the wire under test. It also detected the response of the wire and followed an algorithm for quickly locating the frequency of maximum response.

A set of analog multiplexer chips (MUXes) controlled which of 64 wires was under test. Three digital lines were

* Corresponding author. Tel. +1 412 268 5177, fax +1 412 681 0648, e-mail reinhard@ernest.phys.cmu.edu.

[1] Present address: Cycle Time Corp. Suite 313, 700 River Ave., Pittsburgh, PA 15212, USA.

SSDI 0168-9002(95)00783-0

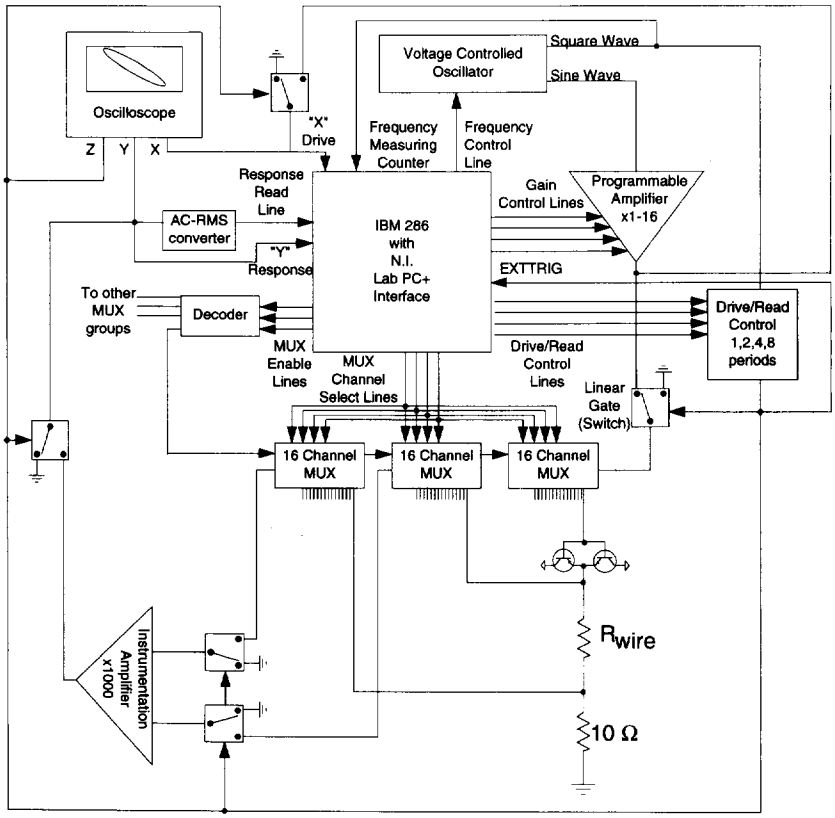

Fig. 1. Block diagram showing the elements of the system. Only one test wire is shown, labeled R_{wire}. Altogether 64 wires were under test. The custom-built portion of the system was installed in a 19 in. rack-mount chassis; the PC-compatible computer and oscilloscope were separate.

decoded to enable one group of three 16-channel MUXes, while four more lines selected the enabled channel. Control of each wire always required three MUX channels for driving and reading.

A single-chip voltage controlled oscillator (VCO) produced both square-wave and sinusoidal signals to drive the circuit. The LabPC+ board could not directly produce the chopped audio frequency signal we needed. The VCO output was calibrated by measuring the frequency with one of the counter inputs on the I/O board. A second order polynomial was very adequate for the voltage vs. frequency calibration. The sinusoidal driving voltage was amplified by a programmable amplifier with gains of 1, 2, 4, 8, or 16.

To switch the circuit from driving a wire to measuring its response, a set of linear gates toggled the test wire connections from the programmable (driving) amplifier to the instrumentation (reading) amplifier. A programmable divide-by-N circuit selected the lengths of the driving and reading periods, which were always equal, and could be $N = 1$, 2, 4, or 8 periods of the driving frequency.

The wire vibrating in the magnetic field produced an induced voltage whose amplitude was on the order of a mV. This signal was sent to the instrumentation amplifier which had a fixed gain of 1000. The output of the amplifier was passed on to an AC-to-RMS converter to obtain a DC signal whose amplitude was proportional to the RMS of the input. This DC signal was sent to an ADC input. The ADC was triggered to start conversions during the beginning of the response cycle. In addition, the AC response signal and the drive signal were directly entered into another pair of ADCs for sensing the relative phase of the drive and response.

The user of this system could watch the computer's progress with an oscilloscope. The X input of the scope showed the driving wave, and the Y input showed the amplified induced voltage across the wire. The Z input was used so the trace was turned off or blanked during the driving cycle.

A detailed circuit diagram is shown in Fig. 2. The analog control voltage from a DAC (pin 10) was conditioned by two op-amps so the full 0–10 V range of the DAC corresponded to the input range of the VCO. The symmetry of the sine and square waves could be set by 100 kΩ and 1 kΩ potentiometers. The precise VCO frequency was measured by counting (at pin 48) cycles of the

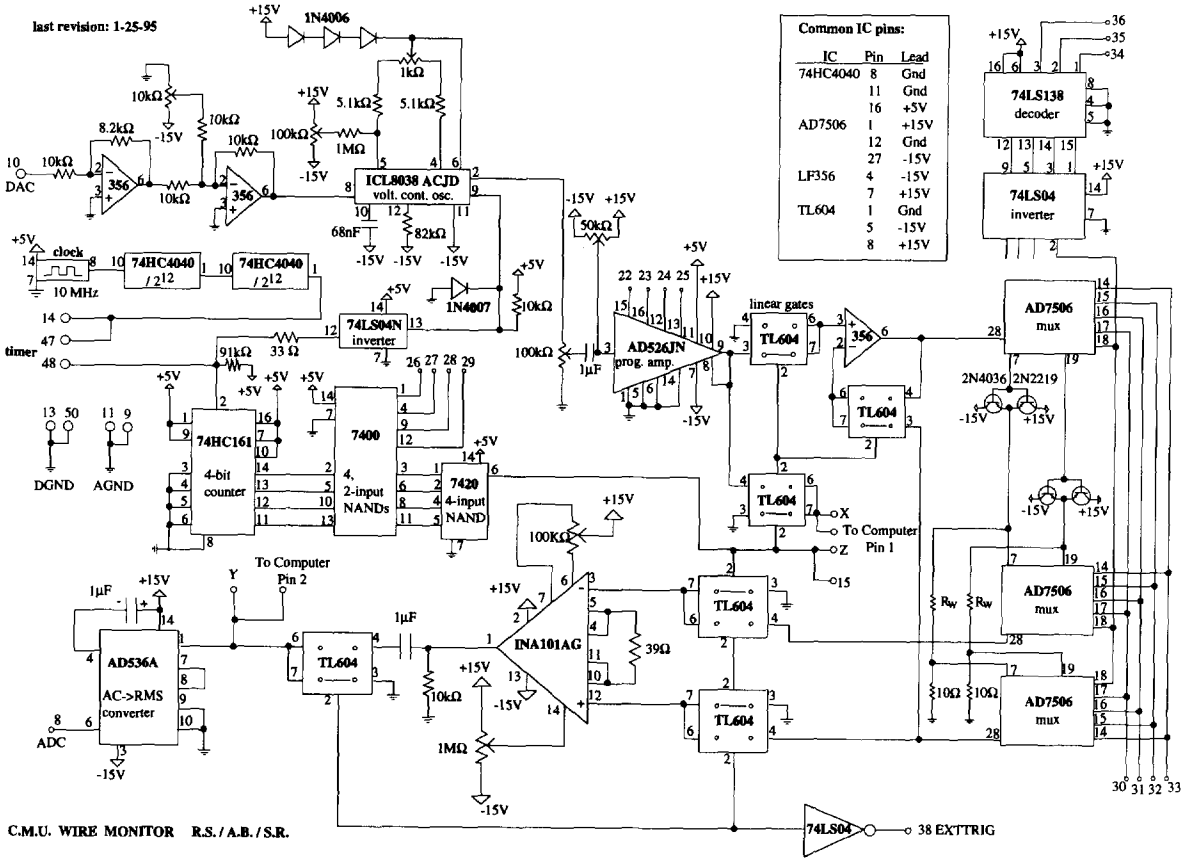

Fig. 2. Full circuit diagram of the wire monitor system. Pin numbers are given for the chips and/or the NI Lab-PC+ board. Two representative test wires labeled R_w are shown, together with one quarter of the MUX circuitry. The linear gates (TL604) are shown as set for driving the test wire with current.

square wave in a time (0.838 s) determined by a divided-down 10 MHz clock (pins 14, 47). A diode, 10 kΩ resistor and the 74LS04 inverter made the square wave TTL compatible. The amplitude of the VCO's sine output was AC coupled to the input of the AD526 programmable amplifier; a 100 kΩ potentiometer matched the input signal to the largest amplifier output. The drive/read control signal was fashioned from the VCO's square wave. A 74HC161 four-bit counter increased the period of the square wave by factors of 2, 4, 8, and 16. The 7400 and 7420 NAND gates were used to pass one of these signals to the circuit.

The analog MUXes controlled which wire was under test. Each MUX chip had a common analog input and 16 digitally selectable outputs. A total of seven digital output lines (pins 30–36) controlled which one of 64 MUX channels was enabled.

Current to the selected wire was supplied by a push-pull transistor pair. Cross-over distortion was small since the transistors were part of the op-amp feedback loop formed by the 356 op-amp, transistors, test wire, MUXes, and linear gates. RMS currents of up to 250 mA were present when the wire was short-circuited ($R_{\text{wire}} = 0$), hence the need for the transistors. The 10 Ω resistors to ground limited the maximum current.

Responses were read by switching the wire by way of the third set of MUX chips to the input of a high quality instrumentation amplifier (INA101AG) which had a gain of 1000. The resulting signal was in the range of 1 V. It was AC coupled and chopped with a linear gate to eliminate spurious offsets. Before the response was passed to the computer it was conditioned by a pair of op-amps (not shown in the figure) so the maximum range in response corresponded to the maximum range of the ADCs. The AC signal was applied directly to an ADC (pin 2), but also converted to rms DC and applied to a second ADC (pin 8). There was similar treatment of the driving voltage leading to pin 1.

Each test wire in this system had its own pair of driver transistors. An alternative design with only one transistor

pair and one less set of MUX chips proved unworkable due to the large resistance (200 Ω) of each channel of the MUXes. The large IR drop in the MUX channels saturated the driving circuitry already at low driving currents. This necessitated removing the MUX chips from the high-current part of the design.

3. Results

In the development of this system the magnetic field was provided by either a small permanent magnet placed in the middle of the wire or by a large electromagnetic coil to cover the whole wire. The small permanent magnet allowed the 1st, 3rd, 5th, and other odd harmonics to be seen, as shown in Fig. 3a. These harmonics had an antinode at the center of the wire where the magnetic field was concentrated, while the 2nd, 4th and other even harmonics had a node in the middle and therefore were not excited. The large coil produced an even magnetic field across the wire so only the first harmonic was present as seen in Fig. 3b. In actual use we were only interested in the first harmonic so the final system typically used the coil.

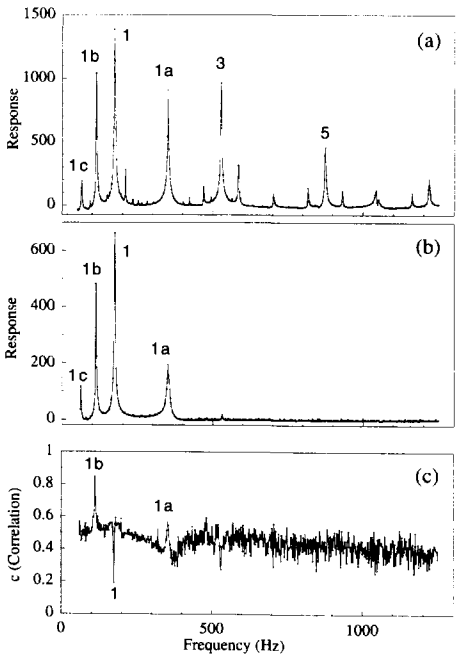

Fig. 3. Response (arbitrary units) vs. frequency (Hz) for a 68.9 cm tungsten wire. (a) A small permanent magnet at the middle of the wire was used to produce the magnetic field. The largest peak, labeled 1, is at the fundamental frequency. The third and fifth harmonics are also excited. The satellite peaks 1a, 1b, 1c, etc., are due to Fourier components of the total driving waveform exciting the first harmonic. $N = 1$ for these data. (b) With a large uniform field only the first harmonic (1) and its satellite peaks (1a, 1b, 1c) are excited. $N = 1$ for these data. (c) To discriminate response at the fundamental frequency from the satellite excitations, a phase correlation parameter called c was used, as discussed in the text.

In Fig. 3 there are additional peaks in the spectrum caused by Fourier components of the driving waveform caused by interruption of the driving signal in order to read the response. Let N be the number of driving oscillations per drive/read cycle, and T the period of the driving oscillations. In the data for Fig. 3 we used $N = 1$. For illustration, wave forms applied to a wire shown in Fig. 4 have $N = 1$ and $N = 2$; note that these even functions can be expanded in cosines alone. We find

$$A(t) + \sum_{m=1}^{\infty} a_m \cos\left(m \frac{\pi}{2} \frac{t}{T}\right), \tag{2}$$

$$a_m = \begin{cases} \frac{1}{\pi}\left[\frac{(-1)^{(2N+m-1)/2}}{2N+m} + \frac{(-1)^{(2N-m-1)/2}}{2N-m}\right] & m = \text{odd}, \\ 0 & m = \text{even} \neq 2N, \\ \frac{1}{2} & m = 2N. \end{cases} \tag{3}$$

These Fourier components produce a rich spectrum of observed peaks when the wire can oscillate at one or more of its harmonics. The wire responded whenever any harmonic of the driving frequency matched the fundamental (or other available) harmonic of the wire. For a permitted wire oscillation frequency f_w, a peak in the response spectrum is seen in Fig. 3a or 3b whenever the driving frequency f_d satisfied

$$f_d = f_w \frac{2N}{m}, \tag{4}$$

where m is odd or equal to $2N$. For $N = 1$ we see $f_d = 2f_w$, $1f_w$, $\frac{2}{3}f_w$, and $\frac{2}{5}f_w$ at peaks 1a, 1, 1b, and 1c, respectively. Fortunately the fundamental peak at $f_d = f_w$ is always largest, although not by much compared to nearly "satellite" peaks. Using the small magnet centered on the wire we also see peaks in Fig. 3a corresponding to the 3rd and 5th harmonics of the wire, plus all the satellite peaks of

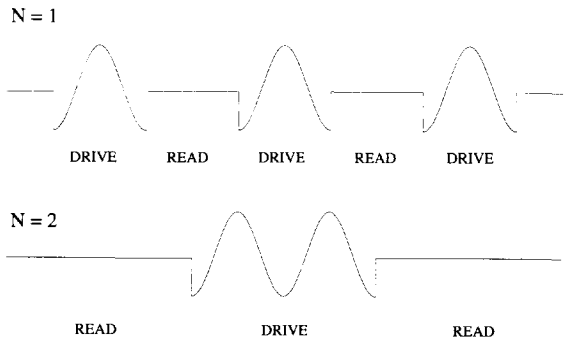

Fig. 4. The waveform used for driving the wires. N is the number of periods of the driving frequency per driving cycle. In this example $N = 1$ (top) and $N = 2$ (bottom).

those harmonics as given by Eq. (4). Peak 1a contains strength from satellite peaks of all the available wire harmonics; in Fig. 3b where the large magnet suppressed the higher wire harmonics, peak 1a is reduced to the contribution from the wire's fundamental frequency alone. The calculated Fourier components for $N = 1$ are 0.5 for peak 1, then 0.21, 0.38, and 0.15 for peaks 1a, 1b, and 1c, respectively, in good qualitative agreement with the data in Fig. 3b.

To avoid the possible confusion caused by these satellite peaks two remedies were found. First, the amplitude of the fundamental vibration was always the largest, so a complete scan of frequencies revealed the fundamental based on amplitude alone. Second, the driving current and induced response voltage in this system were exactly 180° out of phase when the system was driven at any of the wire harmonics. As shown above, the satellite peaks had rational number ratios of drive to response frequency. On the oscilloscope this was easily seen as stable Lissajous patterns. A measure of this frequency ratio was extracted from the AC signals recorded by the computer. Pairs of drive and response data (x_i, y_i) were sampled randomly n times during several cycles, and the data were normalized to have values between -1 and $+1$. The correlation sum defined by

$$c = \frac{1}{n}\sum_i d_i = \frac{1}{n}\frac{1}{\sqrt{2}}\sum_i (x_i + y_i) \tag{5}$$

was formed, where d_i was the perpendicular distance between the ith data point and a line passing through the origin with a slope of -1. For off-resonance situations, when the drive voltage was sinusoidal but the response was completely small and uncorrelated, it is straightforward to show that this sum is $c = \sqrt{2}/\pi = 0.45$. On a harmonic of the wire the sum is equal to zero because of the exact linear correlation between signal and response. For any of the satellite peaks the sum turns out to be greater than 0.45 due to the tendency for the response signal to be "further away" when in phase with the drive signal than for the uncorrelated off-resonance signal. Fig. 3c shows the value of c as a function of frequency. It is a minimum at the resonant peak, while at the satellite peaks labeled 1a and 1b there are values greater than 0.45. With these two methods it was easily possible to distinguish the fundamental vibrations from the response caused by the chopping of the drive signal.

To precisely locate the resonant frequency of a wire, the computer recorded eleven data points around the resonance and fit this data to a Lorentzian with a constant offset. Fig. 5 shows a typical data set and the fit obtained; note that the error bars are comparable in size to the symbols. The reproducibility of the measurements was investigated. Fig. 6b shows a histogram of the tension on a 75.8 cm tungsten wire measured repeatedly over a 20 minute period. The standard deviation of these data is 0.05 g. This remarkably

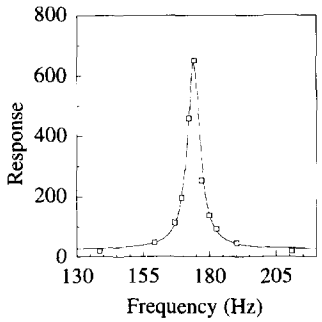

Fig. 5. Typical 20 μm tungsten wire response as a function of frequency together with a Lorentzian fit. Uncertainties on data points, computed from the standard deviations of repeated measurements at each frequency, are smaller than the squares.

small error is due to the very stable nature of the resonant frequency in the tungsten wires. When we used aluminum wires the resonant frequency was not as stable. Fig. 6a shows a similar histogram for a 75.8 cm aluminum wire. The standard deviation of these data is 1.1 g, showing that the reproducibility of the tension measurement on aluminum wires was less than on the tungsten wires. Stability tests showed that currents of air surrounding the wires led to fluctuations in temperature, and therefore in the tension, on time scales from minutes to days.

An effect which limited the accuracy of our system, and presumably of all similar tension monitors, was wire heating due to the driving current. The power dissipated in the wire heated the wire and tended to reduce the measured tension. We investigated this effect and found a simple model to explain the results. Fig. 7 shows the change in tension, in g, as a function of the driving current in mA. The data shown are for 75 μm copper wire, 100 μm aluminum wire, and 20 μm tungsten wire. Note that the decrease in tension goes quadratically with current, suggesting a dependence on the amount of power dissipated in the wire. A wire is characterized by its length L, cross sectional area A, resistivity ρ, thermal expansion coefficient α, Young's modulus Y, and thermal conductivity k. The change in tension of the wire, ΔF, is related to a rise in average temperature, ΔT, caused by the resistive heating. ΔF is related to the Young's modulus and the effective strain:

$$Y = \frac{\text{stress}}{\text{strain}} = \frac{\Delta F/A}{\Delta L/L}. \tag{6}$$

In the present case the strain is caused by the temperature change, so that

$$\Delta L/L = \alpha \Delta T. \tag{7}$$

Thus we may write

$$\Delta F = YA\alpha\Delta T. \tag{8}$$

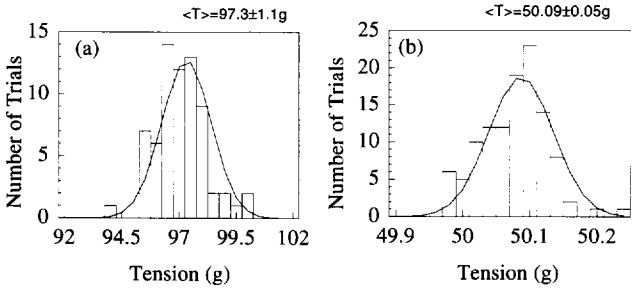

Fig. 6. Reproducibility of tension measurements for two 75.8 cm wires. (a) Histogram of the tension on a 100 μm aluminum wire taken over a 20 minute period of time. The standard deviation of such data was used to estimate the measurement reliability for aluminum wires. (b) Histogram of the tension on a 20 μm tungsten wire; the smaller σ value shows the greater reliability of measurements using tungsten.

The average temperature rise, ΔT, is proportional to the rate of conductive or convective cooling, while the cooling is equal to the rate of energy input, P from resistive heating. In our simple model, which assumes the dominance of conduction over convection, we have

$$P = I^2R = I^2\rho\frac{L}{A} = CLk\Delta T\,, \tag{9}$$

where C is a geometrical constant that ought to be the same for all types of wire. In this picture the heat is conducted to the surface and dissipated at a fixed rate proportional to ΔT, such that thick and thin wires have the same average temperature rise for a given P. If velocity-dependent convection were to dominant the energy dissipation mechanism, the maximum velocity of the wire would scale as the driving force, which is proportional to the current, I. In that case ΔT would go as I instead of I^2, in disagreement with our observations. Thus we expect to find

$$\Delta F = \alpha\rho Y\frac{1}{Ck}I^2\,. \tag{10}$$

The curves in Fig. 7 show the results; a single value of C was used for copper and tungsten, while the C needed to fit the aluminum wire data was about twice as large. Measurements of α, ρ, and Y for our particular aluminum wire disagreed with handbook values, while k was not measurable by us. The departures from the handbook values all improved the agreement with our data, with uncertainties large enough to easily accommodate our measured values. As a result we believe the different value for C for the aluminum case was due to the material properties of our wire, and not a deficiency of our model. In any case, the I^2 dependence of the tension loss seems to be understood.

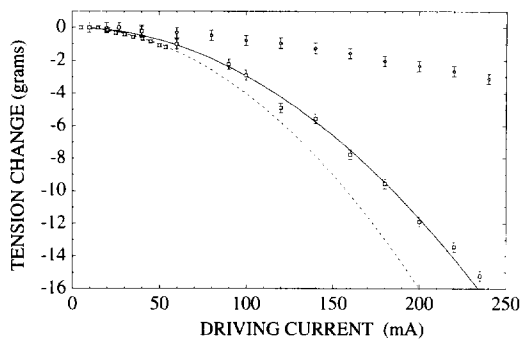

Fig. 7. Sensitivity of the tensions of three types of wire as a function of rms current. The lines are for a model that considers Ohmic heating and conductive cooling. The cases are 100 μm aluminum (squares, solid line), 20 μm tungsten (circles, dashed line), and 75 μm copper (diamonds, dotted line).

4. Operational experience

In actual practice the operation of this system was controlled by a C program, and the user interface was created by NIDAQ LAB Views, a Windows-type of user interface [3]. A database file containing the historical high, low, and most recent measurement for each wire was maintained, along with data giving fit parameters for the resonant peak for each wire. While scanning, the system dwelled typically for 30 seconds on each wire. First it hopped back and forth near the last known resonant frequency for a given wire to find the approximate location of the peak. Then the system made nine measurements of the peak shape using estimates of the peak width as a guide to the step size. A fit to a Lorentzian line shape with a linear background was made and recorded. Suitable alarms to the user were enabled if the wire was not in the desired range. Figs. 3 and 5 showed typical response curves. The speed of the scan was determined by the time between setting a new driving frequency and the wire oscillation stabilizing to the point where a reliable response reading could be obtained. We found this time to be about 1.0 s, although further software tuning may reduce this number significantly.

The resonant response of our shortest wires (about 10 cm in length) was found to be unstable at high values of the drive current (about 200 mA). When scanning over a resonance the amplitude would build to a maximum and

then suddenly collapse to near zero. After some seconds the amplitude would spontaneously build up again. Reducing the drive current always made this problem disappear. The cause of this effect was thought to be related to the temporary tension change due to resistive heating, as discussed above, coupled with small changes in the convective cooling of the wire due to its motion at large values of the driving current. That is, build-up at large current of a large oscillation caused increased convective cooling, which tended to raise the tension and therefore move the wire off its resonance. Once off resonance the wire again heated, relaxed, and started to oscillate, all in a somewhat unstable way. This effect was never observed in wires longer than about 10 cm, and for the short wires decreasing the drive current eliminated the problem.

5. Concluding remarks

This system is in use in the construction (1995 – 6) of the "Region One" drift chamber for the CLAS spectrometer, and will be a permanent monitor of this detector once it is installed and running at CEBAF. About 60 dedicated wires situated throughout the chamber will be used for this purpose. The system described here was already used successfully in the prototyping stage of the "Region One" drift chamber. It allowed us to quantify the degree of stability of the mechanical wire tensions in this detector as it underwent numerous manipulations during the assembly process.

If we were to rebuild this system we would implement sine-like rather than the cosine-like waves shown in fig. 4. The higher-order Fourier components ($m = 11$ and up) would be 3 to 10 times smaller. The major satellite components would not be reduced, however, so this is a minor point.

Acknowledgements

The circuit drawing [4] for a single-wire, hand controlled circuit from which the present system evolved was provided to us by Mr. Steve Christo. We would like to thank Mr. Gary Wilkin, Mr. Chad Hunter, and Mr. Alan Bentley for their assistance in the construction and operation of the system described here. This work was carried out under DOE contract DE-FG02-87ER40315.

References

[1] CEBAF is the Continuous Electron Beam Accelerator Facility at Newport News, VA, and CLAS are the CEBAF Large Acceptance Spectrometer.
F.J. Barbosa et al., Nucl. Instr. and Meth. A 323 (1992) 191.

[2] Some references featuring various methods of exciting and detecting wire oscillations:
S. Bhadra et al., Nucl. Instr. and Meth. A 269 (1988) 33;
M. Calvetti et al., Nucl. Instr. and Meth. 174 (1980) 285;
R.T. Jones, Nucl. Instr. and Meth. A 269 (1988) 550;
B. Koene and L. Linssen, Nucl. Instr. and Meth. 190 (1981) 511;
R. Stephenson and J.E. Bateman, Nucl. Instr. and Meth. 171 (1980) 337;
N.J. Shenhav, Nucl. Instr. and Meth. A 324 (1993) 551;
I. D'Antone et al., Nucl. Instr. and Meth. A 317 (1992) 155;
M. Cavalli-Sforza et al., Nucl. Instr. and Meth. 124 (1975) 124;
N. Ceci, A. Raino, P. Spinelli and V. Stagno, Rev. Sci. Instr. 62 (1991) 2022;
K.B. Burns et al., Nucl. Instr. and Meth. 171 (1973) 171;
A. Borghesi, Nucl. Instr. and Meth. 153 (1978) 379;
T. Regan, Nucl. Instr. and Meth. 219 (1984) 100;
E.R. Mueller, Nucl. Instr. and Meth. A 281 (1989) 652.

[3] National Instruments Lab board, DIO board, and Lab Windows user interface. National Instruments, 6504 Bridge Point Parkway, Austin, TX 78730-5039, Tel: (512) 794-0100.

[4] Signed P. Dunn and D. Saunders. The history of this circuit is unknown to us.